

## **Reply to Reviewer #2:**

Comments to the Author: This paper documents the PM<sub>2.5</sub> changes as a result of COVID-19 in China. Following my previous comments the authors have made many useful revisions and the paper is much improved. I recommend it **be accepted** subject to the following mainly **minor comments being addressed**. Overall I think my revisions are minor, but they are important:

**1. Figure S1 is very helpful and should be added to the main text. With reference to Figure S1a, the authors should comment on the substantial underestimate of the PM<sub>2.5</sub> in northern China (not just in Beijing) and in the westernmost parts of your figure at 35N, and calculate a normalized mean bias from their figure and add it to the text with a comparison to the number obtained by Dang and Liao (2019).**

**They should also discuss Figure S1b in detail in the text, rather than mentioning it in passing. It shows that on average the 2010 emissions substantially overestimate PM<sub>2.5</sub> everywhere and the 1985 emissions still overestimate PM<sub>2.5</sub>, especially in the south, but agree better with the measurements. This is a good justification for using the 1985 inventory, which the authors should explain at line 119, and then add a substantial new paragraph to the text detailing their evaluation.**

### **Reply:**

Appreciate for your detailed and valuable comments. In terms of the evaluation of GEOS-Chem model, we have **made a more complete description based on your comments and added Figure S1 to the main text as Figure 2.**

(1) Dang and Liao (2019) compared the simulated and observed daily mean PM<sub>2.5</sub> concentrations at the Beijing with a normalized mean bias (NMB) of -9.2%. The simulations in February 2017 in this study substantially underestimated the PM<sub>2.5</sub> in northern China with a normalized mean bias (NMB) of -3.0%. Among them, the NMB in The Beijing-Tianjin-Hebei region was -3.3%. However, in the Fenwei plain (the westernmost parts of the figure at 35N), the underestimation was even more pronounced, with NMB reaching -16.3%.

(2) In North China, Yangtze River Delta and Hubei Province, the correlation coefficients between daily PM<sub>2.5</sub> observations and simulated data under 2010 (1985) emission scenario reached 0.83 (0.82), 0.67 (0.63), and 0.79 (0.73), respectively. The correlation coefficients under 2010 emission scenario were all higher than that under

1985 emission scenario maybe due to the **emissions from each sector in 2010 were more similar to recent years**, which was more reasonable. Therefore, we selected the percentages due to different meteorology between 2020 and 2017 calculated under the 2010 emission scenario, instead of making the selection based on the simulation results of the real PM<sub>2.5</sub> value, which was also **mentioned in the following text** as below.

129 PM<sub>2.5</sub> between each year and 2017 under the same emission scenario divided by the simulated PM<sub>2.5</sub> in 2017. For example, the  
130 percentages due to different meteorology between 2020 and 2017 were 22.1% (21.4%), -1.2% (-0.7%) and 9.0% (8.2%) in  
131 NC, YRD and HB under the low (high) emissions (Fig. S2). **The percentage under 2010 emission scenario was selected as the**  
132 **final percentage because the emissions from each sector in 2010 were more similar to recent years, and thus was more**  
133 **reasonable.** Then, through multiplying the 2017 observation by this percentage, PM<sub>dM</sub> can be quantified in each simulation

The evaluation of the simulated PM<sub>2.5</sub> concentration under 2010 emission and 1985 emission in February 2020 was also introduced in the old version as below. In the revised version, we present this section **as a new and separate paragraph** and give a more detailed evaluation and explanation.

**Revision:**

**Lines 92-98:** The absolute biases were larger in the south of China, which was consistent with Dang and Liao (2019). They also compared the simulated and observed daily mean PM<sub>2.5</sub> concentrations at the Beijing, Shanghai, and Chengdu grids, which had a low bias in Beijing with a normalized mean bias (NMB) of -9.2% and high biases with NMBs of 18.6% and 28.7% in Shanghai and Chengdu, respectively. The simulations in February 2017 in this study substantially underestimated the PM<sub>2.5</sub> in NC with an NMB of -3.0% (Fig. 1a). Among them, the NMB in The Beijing-Tianjin-Hebei region was -3.3%. However, in the Fenwei plain, the underestimation was even more pronounced, with NMB reaching -16.3%.

**Lines 102-109:** In NC, YRD and HB, the correlation coefficients between daily PM<sub>2.5</sub> observations and simulated data under 2010 (1985) emission scenario reached 0.83 (0.82), 0.67 (0.63), and 0.79 (0.73), respectively (Fig.1b), and could capture the maximum and minimum PM<sub>2.5</sub> concentrations..... The correlation coefficients under 2010 emission scenario were all higher than that under 1985 emission scenario maybe due to the emissions from each sector in 2010 were more similar to recent years, which was more reasonable.

**2. Rephrase first sentence: “blew China” is not conventional English. “swept through China” would be OK. In general, the quality of the written English could still be improved significantly in several other places not mentioned below, I recommend the authors seek advice from colleagues if at all possible, or assistance from the copy-editors.**

**Reply:**

Thank you for this detailed suggestions. We have rephrased “blew China” to “swept through China” and checked the quality of the written English of the whole text.

**Revisions:**

**Line 23:** The COVID-19 pandemic devastatingly swept through China in the beginning of 2020.....

**3. Line 50-52 are you referring to the same rebound. Rephrase to avoid repetition.**

**Reply:**

These were **two different rebound**. One was the severe haze events occurring in 2016 December, indicating a rebound of PM<sub>2.5</sub> comparing to 2014-2015, and the other was the rebound of PM<sub>2.5</sub> in winter 2018 comparing to 2017 under the same intensified regional air pollution preventions. We have rephrased the explanation to make it clearer.

**Revision:**

**Lines 43-47:** The continuous low surface wind speed of less than 2ms<sup>-1</sup>, high humidity above 80% and strong temperature inversion lasting for 132h caused the serious haze event in 2016 (Yin and Wang, 2017). In winter 2017, the air quality in North China largely improved; however, the stagnant atmosphere in 2018 resulted in a major PM<sub>2.5</sub> rebound comparing to 2017 by weakening transport dispersion and enhancing the chemical production of secondary aerosols (Yin and Zhang 2020).

**4. Line 92 which aerosol microphysics is used here?**

**Reply:**

According to the official website of GEOS-Chem, in the mechanism we run, these two alternate simulations of aerosol microphysics were both simulated. We have explained in the text.

**Revision:**

**Lines 85-86:** Two alternate simulations of aerosol microphysics are implemented in

GEOS-Chem: the TOMAS simulation (Kodros and Pierce, 2017) and the APM simulation (Yu and Luo, 2009), which were both simulated in the experiments.

**5. Line 103 please be quantitative, add the magnitude of the biases to the text.**

**Reply:**

Dang and Liao (2019) compared the simulated and observed daily mean PM<sub>2.5</sub> concentrations at the Beijing, Shanghai, and Chengdu grids, which had a low bias in Beijing with a normalized mean bias (NMB) of **-9.2%** and high biases with NMBs of **18.6%** and **28.7%** in Shanghai and Chengdu, respectively. We have added the specific biases to the text.

**Revisions:**

**Lines 94-96:** They also compared the simulated and observed daily mean PM<sub>2.5</sub> concentrations at the Beijing, Shanghai, and Chengdu grids, which had a low bias in Beijing with a normalized mean bias (NMB) of -9.2% and high biases with NMBs of 18.6% and 28.7% in Shanghai and Chengdu, respectively.

**6. Line 203 and 206 need to explain how the significance testing was carried out.**

**Reply:**

We use ***t* test** which depends on *t* distribution. According to querying the critical value table of correlation coefficient by reliability and degree of freedom, the critical correlation coefficient that passes the *t* test is obtained. If the calculated correlation coefficient is greater than the critical correlation coefficient, it means passing the significance *t* test of the corresponding reliability. We have explained in the text that we used *t* test to test the significance of correlation coefficients.

**Revision:**

**Line 188:** ..... all of which passed the 95% significance test using *t* test method .....

**Line 191:** ..... exceeding the 99% significance test using *t* test method .....

**7. Line 262 “break-off transportation” needs rephrasing.**

**Reply:**

We have rephrased the “break-off transportation” to “the disruption of transportations”.

***Revision:***

**Line 245:** Because of the disruption of transportations.....

**8. Line 296 “approximation was lack of considering”-> “approximation did not consider”**

***Reply:***

We have changed “approximation was lack of considering” to “approximation did not consider”.

***Revisions***

**Line 275:** .....we must note that this approximation did not consider the meteorology-emission interactions.....

**9. The word ‘conjecture’ is inappropriate, I would comment that the technique introduces uncertainty.**

***Reply:***

We have changed “conjecture” to “**estimated value**”, which could show our meaning appropriately.

***Revision:***

**Line 280:** .....it is still estimated value rather than true value.....

**10. Figure 1b caption: specify time period for ratios**

***Reply:***

The time period for ratios is **until the end February**. We have specified it in the caption.

***Revisions:***

**Line 450:** .....(b) The ratio of work resumption in large industrial enterprises in the east of China until the end February.....

# Evident PM<sub>2.5</sub> Drops in the East of China due to the COVID-19 Quarantines in February

Zhicong Yin<sup>123</sup>, Yijia Zhang<sup>1</sup>, Huijun Wang<sup>123</sup>, Yuyan Li<sup>1</sup>

<sup>1</sup>Key Laboratory of Meteorological Disaster, Ministry of Education / Joint International Research Laboratory of Climate and Environment Change (ILCEC) / Collaborative Innovation Center on Forecast and Evaluation of Meteorological Disasters (CIC-FEMD), Nanjing University of Information Science & Technology, Nanjing, 210044, China

<sup>2</sup>Southern Marine Science and Engineering Guangdong Laboratory (Zhuhai), Zhuhai, 519080, China

<sup>3</sup>Nansen-Zhu International Research Centre, Institute of Atmospheric Physics, Chinese Academy of Sciences, Beijing, China

Correspondence to: Zhicong Yin (yinzhc@163.com)

**Abstract.** The top-level emergency response to the COVID-19 pandemic involved an exhaustive quarantine in China. The impacts of COVID-19 quarantine on the decline in fine particulate matter (PM<sub>2.5</sub>) were quantitatively assessed based on numerical simulations and observations in February. Relative to both of February 2017 and climate mean, anomalous southerlies and moister air occurred in the east of China in February 2020, which caused considerable PM<sub>2.5</sub> anomalies. Thus, it is a must to disentangle the contributions of stable meteorology from the effects of the COVID-19 lockdown. The contributions of routine emission reductions were also quantitatively extrapolated. The top-level emergency response substantially alleviated the level of haze pollution in the east of China. Although climate variability elevated the PM<sub>2.5</sub> by 29% (relative to 2020 observations), 59% decline related to COVID-19 pandemic and 20% decline from the expected pollution regulation dramatically exceeded the former in North China. The COVID-19 quarantine measures decreased the PM<sub>2.5</sub> in Yangtze River Delta by 72%. In Hubei Province where most pneumonia cases were confirmed, the impact of total emission reduction (72%) evidently exceeded the rising percentage of PM<sub>2.5</sub> driven by meteorology (13%).

**Keywords:** COVID-19, PM<sub>2.5</sub>, Emission Reduction, Climate Variability, Haze

## 1 Introduction

The COVID-19 pandemic devastatingly [blew swept through](#) China in the beginning of 2020 (Luo, 2020; Xia et al., 2020; Cao et al., 2020). By April 2020, more than 84 thousand confirmed cases were reported by the National Health Commission of China, approximately 75% of which were confirmed in February (Fig. 1a). To effectively control the large spread of COVID-19 pneumonia, stringent quarantine measures were implemented by the Chinese government and people themselves, including prohibiting social activities, shuttering industries, stopping transportation, etc. (Chen S. et al., 2020). The abovementioned emergency response measures were first carried out in Wuhan on 23 January, which resulted in the delayed arrival of COVID-19 in other cities by 2.91 days, and these response measures were in effect in all cities across China, thus limiting the spread of the COVID-19 epidemic in China (Tian et al., 2020). Since March 7, the number of newly confirmed cases in China has

31 been nearly below 100. On the other hand, the COVID-19 quarantine measures greatly reduced anthropogenic emissions, and  
32 therefore, the air quality in China was considerably improved (Wang et al., 2020). Chen K. et al. (2020) simply compared  
33 observations of atmospheric components before and during the quarantine and found that the concentration of fine particulate  
34 matter (PM<sub>2.5</sub>) in Wuhan decreased 1.4 μg/m<sup>3</sup>, but it decreased 18.9 μg/m<sup>3</sup> in 367 cities across China. Shi et al. (2020) quantified  
35 a 35% reduction of PM<sub>2.5</sub> on average during the COVID-19 outbreak compared to the pre-COVID-19 period. Huang et al.  
36 (2020) used comprehensive measurements and modeling to show that the haze during COVID-19 lockdown was driven by  
37 enhancements of secondary pollution, which offset reduction of primary emissions during this period in China. However, the  
38 impacts of meteorology on the air quality were neglected in many previous studies.

39 Climate variability notably influences the formation and intensity of haze pollution in China (Yin and Wang 2016; Xiao  
40 et al., 2015; Zou et al., 2017), and the impacts are embodied by variations in surface wind, boundary layer height and moisture  
41 conditions (Shi et al., 2019; Niu et al., 2010; Ding et al., 2014). During December 16th-21st 2016, although most aggressive  
42 control measures for anthropogenic emissions were implemented, severe haze pollution with PM<sub>2.5</sub> concentrations ≈ 1100μg  
43 m<sup>-3</sup> still occurred and covered 710,000km<sup>2</sup>. The continuous low surface wind speed of less than 2ms<sup>-1</sup>, high humidity above  
44 80% and strong temperature inversion lasting for 132h caused the ~~rebound of serious haze event wintertime PM<sub>2.5</sub>~~ in 2016  
45 (Yin and Wang, 2017). In winter 2017, the air quality in North China largely improved; however, the stagnant atmosphere in  
46 2018 resulted in a major PM<sub>2.5</sub> rebound ~~comparing to 2017~~ by weakening transport dispersion and enhancing the chemical  
47 production of secondary aerosols (Yin and Zhang 2020). Wang et al. (2020) applied the Community Multiscale Air Quality  
48 model to emphasize that the role of adverse meteorological conditions cannot be neglected even during the COVID-19  
49 outbreak. From February 8 to 13 2020, North China suffered severe pollutions, with maximum daily PM<sub>2.5</sub> exceeding 200μg  
50 m<sup>-3</sup>. During this period, weak southerly surface winds lasted for nearly 5 days, relative humidity was close to 100%, and  
51 atmospheric inversion reached more than 10°C. Although pollution emissions from basic social activities have been reduced,  
52 heavy pollution still occurred when adverse meteorological conditions characterized by stable air masses appeared (Wang et  
53 al., 2020).

54 After the severe haze events of 2013, routine emission reductions resulted in an approximately 42% decrease in the annual  
55 mean PM<sub>2.5</sub> concentration between 2013 and 2018 in China (Cleaner air for China, 2019). In November 2019, the Ministry of  
56 Environmental Protection of China issued a series of Autumn-Winter Air Pollution Prevention and Management Plans  
57 indicating that the routine emission reductions would be conventionally implemented in the following winter (Ministry of  
58 Environmental Protection of China, 2019). As reported by the government, the mean ratio of work resumption in large  
59 industrial enterprises was approximately 90% in the east of China until the end of February (Fig. 1b). In this study, we attempted  
60 to quantify the impacts of the COVID-19 pandemic on the observed PM<sub>2.5</sub> concentration in February 2020 when the quarantine  
61 measures were the strictest. The official 7-day Chinese New Year holiday occurs in January and February and commonly  
62 accounts for approximately 25% of a month. From 2013–2020, there were only two years (2017 and 2020) when the official

63 7-day holiday occurred in January (Fig. 1c). Thus, to avoid the impacts of the Spring Festival, the observed PM<sub>2.5</sub> concentration  
64 in February 2017 (Fig. 1a) was adopted to calculate the PM<sub>2.5</sub> difference, which was decomposed into the results due to  
65 expected routine emission reductions, changing meteorology climate variability, and COVID-19 quarantines.

## 66 2 Datasets and methods

### 67 2.1 Data description

68 Monthly mean meteorological data from 2015 to 2020 were obtained from NCEP/NCAR reanalysis datasets, with a  
69 horizontal resolution of 2.5°×2.5°, including the geopotential height at 500 hPa (H500), zonal and meridional winds at 850  
70 hPa, vertical wind from the surface to 150 hPa, and relative humidity at the surface (Kalnay et al., 1996). PM<sub>2.5</sub> concentration  
71 data from 2015 to 2020 were acquired from the China National Environmental Monitoring Centre (<https://quotsoft.net/air/>).  
72 The monitoring network expanded from 1500 sites in 2015 to 1640 sites in 2020, covering approximately 370 cities nationwide.  
73 The PM<sub>2.5</sub> data were monitored every 5 min using two methods: a tapered element oscillating microbalance and β-rays, which  
74 were operated under the China National Quality Control.

### 75 2.2 GEOS-Chem description, evaluation and experimental design.

76 We used the GEOS-Chem model (<http://acmg.seas.harvard.edu/geos/>) to simulate the PM<sub>2.5</sub> concentration, driven by  
77 MERRA-2 assimilated meteorological data (Gelaro et al., 2017). The nested grid over China (15° N–55° N, 75–135° E) had a  
78 horizontal resolution of 0.5° latitude by 0.625° longitude and consisted of 47 vertical layers up to 0.01 hPa. The GEOS-Chem  
79 model included the fully coupled O<sub>3</sub>–NO<sub>x</sub>–hydrocarbon and aerosol chemistry module with more than 80 species and 300  
80 reactions (Bey et al., 2001; Park et al., 2004). The PM<sub>2.5</sub> components simulated in the GEOS-Chem model included sulfate,  
81 nitrate, ammonium, black carbon and primary organic carbon, mineral dust, and sea salt. Aerosol thermodynamic equilibrium  
82 is computed by the ISORROPIA package, which calculates the gas–aerosol partitioning of the sulfate–nitrate–ammonium  
83 system (Fountoukis and Nenes, 2007). Heterogeneous reactions of aerosols include the uptake of HO<sub>2</sub> by aerosols (Thornton  
84 et al., 2008), irreversible absorption of NO<sub>2</sub> and NO<sub>3</sub> on wet aerosols (Jacob, 2000), and hydrolysis of N<sub>2</sub>O<sub>5</sub> (Evans and Jacob,  
85 2005). Two alternate simulations of aerosol microphysics are implemented in GEOS-Chem: the TOMAS simulation (Kodros  
86 and Pierce, 2017) and the APM simulation (Yu and Luo, 2009), which were both simulated in the experiments.

87 GEOS-Chem model has been widely used to examine the historical changes in air quality in China and quantitatively  
88 separate the impacts of physical-chemical processes. Using the GEOS-Chem model, Yang et al. (2016) found an increasing  
89 trend of winter PM<sub>2.5</sub> concentrations during 1985–2005, 80% of which due to anthropogenic emissions and 20% due to  
90 meteorological conditions. Here, we simulated the PM<sub>2.5</sub> concentrations in February 2017 and evaluated the performance of  
91 GEOS-Chem (Fig. S42a). The values of mean square error / mean equals were 5.8%, 7.0% and 5.4% in North China (NC),



92 Yangtze River Delta (YRD) and Hubei Province (HB), respectively, indicating the good performance of reproducing the haze-  
93 polluted conditions. The absolute biases were larger in the south of China, which was consistent with Dang and Liao (2019).  
94 They also compared the simulated and observed daily mean PM<sub>2.5</sub> concentrations at the Beijing, Shanghai, and Chengdu grids,  
95 which had a low bias in Beijing with a normalized mean bias (NMB) of -9.2% and high biases with NMBs of 18.6% and 28.7%  
96 in Shanghai and Chengdu, respectively. The simulations in February 2017 in this study substantially underestimated the PM<sub>2.5</sub>  
97 in NC with an NMB of -3.0% (Fig. 2a). Among them, the NMB in The Beijing-Tianjin-Hebei region was -3.3%. However, in  
98 the Fenwei plain, the underestimation was even more pronounced, with NMB reaching -16.3%. The simulated biases possibly  
99 affected the subsequent results and brought uncertainties to some extent. The simulated spatial distribution of PM<sub>2.5</sub> was also  
100 similar to that of observations with spatial correlation coefficient = 0.78.

101 We further verified whether the simulations could capture the roles of meteorological changes in February 2020 under a  
102 substantial reduction in emissions because of COVID-19 quarantines. In NC, YRD and HB, the correlation coefficients  
103 between daily PM<sub>2.5</sub> observations and simulated data under 2010 (1985) emission scenario reached 0.83 (0.82), 0.67 (0.63),  
104 and 0.79 (0.73), respectively (Fig. 2b-d), and could capture the maximum and minimum PM<sub>2.5</sub> concentrations. For example,  
105 in NC, the simulation could well simulate severe haze events (e.g., from 8–13 and 19–25 February) and good air quality events  
106 (e.g., from 14–18 February), reflecting that it has ability to accurately capture the change of meteorological conditions (Fig-  
107 S1b). The correlation coefficients under 2010 emission scenario were all higher than that under 1985 emission scenario maybe  
108 due to the emissions from each sector in 2010 were more similar to recent years, which was more reasonable.

109 The PM<sub>2.5</sub> concentration in February from 2015 to 2020 was simulated in this study. Due to delayed updates of the  
110 emission inventory, we used the emissions data of 2010  
111 (<http://geoschemdata.computecanada.ca/ExtData/HEMCO/AnnualScalar>) and 1985 (M. Li et al., 2017) for the simulations,  
112 which represented high- and low-emission scenarios, respectively. In total, we conducted two sets of numerical experiments  
113 to drive the GEOS-Chem simulations, one combining the meteorological conditions from 2015 to 2020 with fixed emissions  
114 in 1985 and the other with fixed emissions in 2010, which could determine the stability of simulated results.

### 115 **2.3 The method to quantify the influence of the COVID-19 quarantine.**

116 As mentioned above, we aimed to examine the impact of the COVID-19 quarantines on PM<sub>2.5</sub> over the February 2017  
117 level basing on an observational-numerical hybrid method. The observed PM<sub>2.5</sub> difference in February 2020 (PMd<sub>OBS</sub>) was  
118 linearly decomposed into three parts: the impacts of changing meteorology (PMd<sub>M</sub>), expected routine emissions reductions  
119 (PMd<sub>R</sub>) and COVID-19 quarantines (PMd<sub>C</sub>), which was a reasonable approximation, and the decomposition equation was  
120  $PMd_{OBS} = PMd_M + PMd_R + PMd_C$ . That is,  $PMd_C = PMd_{OBS} - PMd_M - PMd_R$ . It should be noted that PMd<sub>C</sub> is the impact of  
121 the COVID-19 quarantines over the situation whereby the pandemic did not occur and routine emission reductions  
122 conventionally were in effect. The value of PMd<sub>E</sub> (i.e., PMd<sub>R</sub> + PMd<sub>C</sub>) was the total impact of the emission reductions in

123 February 2020 over the 2017 level.

124 Simulated  $PM_{2.5}$  data driven by changing meteorology with two fixed-emissions (1985 and 2010) were employed to  
125 determine the ratio of  $PMd_M$  of each year/ observed  $PM_{2.5}$  in 2017. Depending on the GEOS-Chem simulations, we found that  
126 the percentage of changed  $PM_{2.5}$  due to the differences in meteorology remained nearly constant regardless of the emission  
127 level (Fig. S12), which was consistent with the results of Yin and Zhang (2020). This percentage was the difference of simulated  
128  $PM_{2.5}$  between each year and 2017 under the same emission scenario divided by the simulated  $PM_{2.5}$  in 2017. For example, the  
129 percentages due to different meteorology between 2020 and 2017 were 22.1% (21.4%), -1.2% (-0.7%) and 9.0% (8.2%) in  
130 NC, YRD and HB under the low (high) emissions (Fig. S12). The percentage under 2010 emission scenario was selected as  
131 the final percentage because the emissions from each sector in 2010 were more similar to recent years, and thus was more  
132 reasonable. Then, through multiplying the 2017 observation by this percentage,  $PMd_M$  can be quantified in each simulation  
133 grid with respect to 2017 (STEP 1).

134 From 2015 to 2019,  $PMd_C = 0$ ; thus,  $PMd_R = PMd_{OBS} - PMd_M$ . Here, we repeated STEP 1 to determine  $PMd_M$  in each year  
135 from 2015 to 2019 relative to 2017 (i.e.,  $PMd_M = 0$  in 2017). After removing the effect of meteorological conditions in  $PM_{2.5}$   
136 differences,  $PMd_R$  in all years except 2020 can also be calculated. According to many previous studies, the change in emissions  
137 resulted in a linear change in air pollution in China from 2013-2019 (Wang et al., 2020; Geng et al., 2020) which might be  
138 related to the huge emission reduction due to the implementation of clean air action. Because the signal of emissions reduction  
139 in China had been particularly strong since 2013, it could be easily detected and the assumption of a linear reduction in  
140 pollution caused by emission reduction was applicable in China in the past few years. Based on this approximation, we used  
141 the method of extrapolation to speculate the impact of routine emission reduction on  $PM_{2.5}$ . We performed linear extrapolation  
142 based on known  $PMd_R$  values from 2015 to 2019 to obtain  $PMd_R$  in 2020 (STEP 2, Fig. S23). This  $PMd_R$  in 2020 was calculated  
143 as the change of  $PM_{2.5}$  caused by expected routine emission reduction, which did not actually happen, but merely gave an  
144 assessment in the case of “if no COVID-19”. In Beijing and Shanghai, for example,  $PM_{2.5}$  fell by 23.1% and 26.6% due to  
145 routine emission reduction in 2019, respectively, compared with 2015. Zhou et al. (2020) indicated that emission reductions  
146 caused 20–26% decreases in winter in Beijing which has been translated into 5 years. Zhang et al. (2020) also showed that the  
147 emission controls in Beijing-Tianjin-Hebei (BTH) region have led to significant reductions in  $PM_{2.5}$  from 2013 to 2017 of  
148 approximately 20% after excluding the impacts of meteorology. Geng et al. (2020) found a 20% drop in the main component  
149 of  $PM_{2.5}$  in the Yangtze River Delta from 2013 to 2017. These results are consistent with our extrapolated results. Therefore,  
150 it is reasonable to obtain  $PMd_R$  by extrapolation after disentangling the effects of meteorological conditions.

151 Through STEP 1 and STEP 2,  $PMd_C$  and  $PMd_R$ , respectively, in 2020 can be determined.  $PMd_{OBS}$  can be directly  
152 calculated from the observed data. After removing the influences of climate anomalies and routine emission reductions, the  
153 impact of COVID-19 quarantines on  $PM_{2.5}$  ( $PMd_C$ ) was extracted as  $PMd_{OBS} - PMd_M - PMd_R$  (STEP 3).

155 The mean PM<sub>2.5</sub> concentration in February 2020 was nearly below 80 µg/m<sup>3</sup> at the vast majority of sites in the east of  
156 China, which was much lower than before (Fig. S34). North China (NC) was still the most polluted region (>40 µg/m<sup>3</sup>), but  
157 the PM<sub>2.5</sub> concentrations in the Pearl River Delta (PRD) and Yangtze River Delta (YRD) were < 20 µg/m<sup>3</sup> and < 40 µg/m<sup>3</sup>,  
158 respectively. Relative to the observations in February 2017, negative PM<sub>2.5</sub> anomalies were centered in NC, with values of  
159 approximately -60 to -40 µg/m<sup>3</sup> in southern Hebei Province and northern Henan Province (Fig. 32). In Hubei Province (HB),  
160 where the COVID-19 pneumonia cases were the most severe in February, the PM<sub>2.5</sub> concentration was 20-40 µg/m<sup>3</sup> lower  
161 than that in 2017. The PM<sub>2.5</sub> differences were also negative in YRD and PRD. Therefore, how much did air pollution decrease  
162 due to the COVID-19 quarantines in February in east of China?

163 Climate variability notably influences the interannual-decadal variations in haze pollution as verified by both  
164 observational analysis (Yin et al., 2015) and GEOS-Chem simulations (Dang and Liao, 2019). Furthermore, Zhang et al. (2020)  
165 reported that meteorology contributes 50% and 78% of the wintertime PM<sub>2.5</sub> reduction between 2017 and 2013 in the BTH  
166 and YRD, respectively. Therefore, it is necessary to disentangle the influences of climate anomalies before quantifying the  
167 contributions of the COVID-19 quarantines on the air quality. The highest observed PM<sub>2.5</sub> concentrations were 274, 223, and  
168 303 µg/m<sup>3</sup> in Beijing, Tianjin and Shijiazhuang, respectively. Although human activities had sharply decreased, severe haze  
169 pollution (e.g., 8-13 and 19-25 February 2020) was not avoided, which was attributed to the stagnant atmosphere (Wang et  
170 al., 2020), and these severe haze events were also reproduced by the GEOS-Chem simulation (see Section 2.2 and Fig. S42b).

171 As shown in Figure 4a-b, the meteorological conditions in February 2020 were more favorable for the occurrence of haze  
172 pollution in NC. In the mid-troposphere, an anomalous anticyclone was located over NC and the Sea of Japan (Fig. 4a). These  
173 anticyclonic anomalies clearly stimulated anomalous southerlies over eastern China, which not only transported sufficient  
174 water vapor to NC but also overwhelmed the climatic northerlies in winter (Fig. 4b). In addition, the anomalous upward motion  
175 associated with anomalous anticyclones prevented the downward transportation of westerly momentum and preserved the  
176 thermal inversion layer over NC (Fig. S45). Particularly, in the stagnant days (i.e., 8-13 and 19-25 February), the East Asia  
177 deep trough, one of the most significant zonally asymmetric circulations in the wintertime Northern Hemisphere (Song et al.,  
178 2016), shifted eastwards and northwards than climate mean, which steered the cold air to North Pacific instead of North China  
179 (Fig. 4c). The climatic northerlies in February, related to East Asia winter monsoon, also turned to be south winds in the east  
180 of China (Fig. 4d). Physically, the weakening surface winds and strong thermal inversion corresponded to weaker dispersion  
181 conditions, and the higher humidity indicated a favorable environment for the hygroscopic growth of aerosol particles to  
182 evidently decrease the visibility. Compared with the climate (February 2017) monthly mean, boundary layer height (BLH)  
183 decreased by 19.5m (34.5m), surface relative humidity (rh<sub>surf</sub>) increased by 5% (10.6%) and surface air temperature (SAT)  
184 rose by 1.6°C (0.9°C) after detrending, which were conducive to the increase of PM<sub>2.5</sub> concentration in February 2020.

185 Furthermore, the correlation coefficients of daily PM<sub>2.5</sub> and BLH, rhum, wind speed and SAT in North China were -0.63, 0.44,  
186 -0.45 and 0.46, respectively, all of which passed the 95% significance test [using t test method](#) and indicated importance of  
187 meteorology. We used the meteorological data in February 2017 to establish a multiple linear regression equation to fit PM<sub>2.5</sub>.  
188 The correlation coefficients between the fitting results and the observed PM<sub>2.5</sub> concentration in NC, YRD and HB reached 0.84,  
189 0.64 and 0.65, exceeding the 99% significance test [using t test method](#). Then, we put the observed meteorological data in  
190 February 2020 into this established multiple regression equation to get the predicted PM<sub>2.5</sub> concentration. Using the regress-  
191 predicted value, the percentage of changed PM<sub>2.5</sub> due to the differences in meteorology between 2017 and 2020 were re-  
192 calculated and is 20.7%, -3.2% and 9.5% in NC, YRD and HB, respectively (Fig. S12), which is consistent with and enhanced  
193 the robustness of the results obtained by our previous model simulation. Based on the GEOS-Chem simulations, PM<sub>dM</sub> was  
194 calculated between February 2020 and 2017 (see Methods). To the south of 30°N, most PM<sub>dM</sub> values were negative with small  
195 absolute values, at < 10 µg/m<sup>3</sup>. To the north of 30°N, the PM<sub>dM</sub> values were mostly positive, ranging from 30~60 µg/m<sup>3</sup> in  
196 BTH (Fig. 53a).

197 Since 2013, the Chinese government has legislated and implemented stringent air pollution prevention and management  
198 policies that have clearly contributed to air quality improvement (Wang et al., 2019). As mentioned above, without the COVID-  
199 19 pandemic, these emission reduction policies would certainly remain in effect in February 2020. Thus, we extrapolated PM<sub>dR</sub>  
200 (i.e., the PM<sub>2.5</sub> difference due to expected routine emission reductions) between February 2020 and 2017 to isolate the impacts  
201 of the COVID-19 quarantines (i.e., PM<sub>dC</sub>). PM<sub>dR</sub> was mostly negative in the east of China (Fig. 53b). Because the impacts of  
202 meteorology were proactively removed, these negative values illustrated that routine emission reductions substantially reduced  
203 the wintertime PM<sub>2.5</sub> concentration. The contributions of the emission reduction policies were the greatest in the south of BTH  
204 and were also remarkable in Hubei Province (Fig. 35b). Although the PM<sub>dR</sub> of Beijing in 2016 did not strictly comply with  
205 the pattern of monotonous decrease, which might be caused by the fluctuation of policy and its implementation, the value of  
206 PM<sub>dR</sub> in 2020 relative to 2017 was -8.4 µg/m<sup>3</sup> and was comparable to the 11.5 µg/m<sup>3</sup> reductions due to policy during 2013–  
207 2017 (Zhang et al., 2020). In Shanghai, PM<sub>dR</sub> was -12.0 µg/m<sup>3</sup> (Fig. 65), whose magnitude was proportional with assessments  
208 by Zhang et al. (2020), and the trend was nearly linear. The rationality of the extrapolations of PM<sub>dR</sub> was also proved in Section  
209 2.3. The trend of PM<sub>dR</sub> in Wuhan was -9.6 µg/m<sup>3</sup> per year from 2015–2019, which indicated high efficiency of the emission  
210 reduction policies and resulted in large PM<sub>dR</sub> values in 2020 (i.e., -21.8 µg/m<sup>3</sup>).

211 By disentangling the impacts of meteorology and routine emission reduction policies, the change in PM<sub>2.5</sub> due to the  
212 COVID-19 quarantines was quantitatively extracted. As expected, this severe pandemic caused dramatic slumps in the PM<sub>2.5</sub>  
213 concentration across China (Fig. 53c). Large PM<sub>dC</sub> values (approximately -60 to -30 µg/m<sup>3</sup>) were located in the high-polluted  
214 NC regions where intensive heavy industries were stopped and the traditional massive social activities and transportations  
215 around Chinese New Year were cancelled as part of the COVID-19 quarantine measures. To the south of 30°N, the impacts of  
216 the COVID-19 quarantines on the air quality were relatively weaker (-30 ~ 0 µg/m<sup>3</sup>) than those in the north. Generally, the

217 south region was less polluted than the north, therefore the baseline of  $PM_{2.5}$  concentration was relatively lower (Fig. S34a).  
218 In addition, meteorological conditions in the south in February 2020 had no positive contribution (Fig. 53a), which would not  
219 lead to the increase of  $PM_{2.5}$  concentration. These two possible reasons resulted in a smaller space for  $PM_{2.5}$  decrease due to  
220 COVID-19 quarantines in the south and accompanying regional differences. To reduce the assessment uncertainties, the  
221 percentage of changed  $PM_{2.5}$  due to the differences in meteorology were recalculated based on the GEOS-Chem simulations  
222 with fixed emission in 1985. As described in the Methods section, the recalculated  $PMd_C$  in Figure S56 were consistent with  
223 those in Figure 53c, showing a high robustness. Furthermore, the mean  $PM_{2.5}$  concentration decreases due to the COVID-19  
224 quarantines in NC, HB and YRD were analyzed, which accounted for 59%, 26% and 72% of the observed February  $PM_{2.5}$   
225 concentration in 2020 (Fig. 76).

226 It should be noted that the sum of  $PMd_R$  and  $PMd_C$  (i.e.,  $PMd_E$ ) is the total contribution of the emission reduction in  
227 February 2020 with respect to 2017 (Fig. 53d). In NC, YRD and HB, the COVID-19 quarantines and routine emission  
228 reductions drove  $PM_{2.5}$  in the same direction. The mean  $PM_{2.5}$  decrease in NC, due to the total emission reduction, was  $-43.3$   
229  $\mu\text{g}/\text{m}^3$ , accounting for 79% of the observed February  $PM_{2.5}$  concentration in 2020 (Fig. 76). Although the absolute values of  
230 both  $PMd_R$  and  $PMd_C$  in YRD were smaller than those in NC, the change percentage (92%) was larger because of the lower  
231 base  $PM_{2.5}$  concentration. In HB, where more than 80% of the confirmed COVID-19 cases in China occurred and the cities  
232 were in emergency lockdown, the total anthropogenic emissions were clearly limited, which resulted in a 72% decline in  $PM_{2.5}$   
233 in the atmosphere (Fig. 76). In particular, if the anthropogenic emissions did not decline, the  $PM_{2.5}$  concentration in NC, YRD  
234 and HB would increase to nearly twice the current observation (Fig. 76), indicating significant contributions of human activities  
235 to the air pollution in China.

236 The declines of  $PM_{2.5}$  seemed not to be directly proportional to the almost complete shutoff of vehicle traffics and  
237 industries, that is, the reduction ratio of  $PM_{2.5}$  concentrations were smaller than that of precursor emissions (Wang et al., 2020).  
238 The unexpected air pollutions during the marked emission reductions were closely related to the stagnant air flow, enhanced  
239 productions of secondary aerosols, and uninterrupted residential heating, power plants and petrochemical facilities (Le et al.,  
240 2020). The partial impacts of stagnant meteorological conditions have been explained earlier (Fig. 4). In Wuhan, the  $PM_{2.5}$   
241 remained the main pollutant during the city lockdown and the high level of sulphur dioxide ( $SO_2$ ) may be related to the  
242 increased domestic heating and cooking (Lian et al., 2020). In North China, large reductions of primary aerosols were observed,  
243 but the decreases in secondary aerosols were much smaller (Sun et al., 2020; Shi et al., 2020). Because of the disruption of  
244 break-off transportations, reduced nitrogen oxide ( $NO_x$ ) increased the concentrations of ozone and nighttime nitrate ( $NO_3$ )  
245 radical formations. The increased oxidizing capacity in the atmosphere enhanced the formation of secondary particulate matters  
246 (Huang et al., 2020). Thus, the non-linear relationship of emission reduction and secondary aerosols also partially contributed  
247 to the haze occurrence during the COVID-19 lockdown.

249 In the beginning of 2020, the Chinese government implemented top-level emergency response measures to contain the  
250 spread of COVID-19. The traditional social activities surrounding Chinese New Year, industrial and transportation activities,  
251 etc. were prohibited, which effectively reduced the number of confirmed cases in China. Concomitantly, anthropogenic  
252 emissions, which are the fundamental reason for haze pollution, were dramatically reduced by the COVID-19 quarantine  
253 measures. In this study, we employed observations and GEOS-Chem simulations to quantify the impacts of the COVID-19  
254 quarantines on the air quality improvement in February 2020 after decomposing the contributions of expected routine emission  
255 reductions and climate variability. Although the specific influences varied by the region, the COVID-19 quarantines  
256 substantially decreased the level of haze pollution in the east of China (Fig. 76). In North China, the meteorological conditions  
257 were stagnant that enhanced the  $PM_{2.5}$  concentration by 30% (relative to the observations in 2020). In contrast, the expected  
258 routine emissions reductions and emergency COVID-19 quarantine measures resulted in an 80% decline. In YRD, the impacts  
259 of meteorology were negligible but the COVID-19 quarantines decreased  $PM_{2.5}$  by 72%. In Hubei Province, the impact of the  
260 total emission reduction (72%) evidently exceeded the  $PM_{2.5}$  increase due to meteorological conditions (13%). In March, due  
261 to the continued control of the COVID-19, the quarantines measures still contributed to the negative anomalies of the observed  
262  $PM_{2.5}$  between 2020 and 2017 (Fig. 87a). Because the activities in production and life have been gradually resumed in March,  
263 the  $PM_{2.5}$  drops caused by the COVID-19 quarantines became weaker compared with February (Fig. 87b, c). The contributions  
264 of  $PM_{DC}$  to the change of  $PM_{2.5}$  concentration in NC, YRD and HB declined from 32.2, 21.0 and 12.1  $\mu\text{g}/\text{m}^3$  in February to  
265 7.0, 2.4 and 6.7  $\mu\text{g}/\text{m}^3$  in March respectively.

266 Because of the common update delay of the emission inventory, we employed a combined analysis consisting of  
267 observational and numerical methods. We strictly demonstrated the rationality of this method and the results, mainly based on  
268 the relatively constant contribution ratio of changing meteorology from GEOS-Chem simulations under the different emissions  
269 (Yin and Zhang 2020). However, there was a certain bias in the simulations by GEOS-Chem model, and the biases also showed  
270 regional differences (Dang and Liao, 2019). Therefore, gaps between the assessed results and reality still exist, which requires  
271 further numerical experiments when the emission inventory is updated. Furthermore, during the calculation process, the  
272 observed  $PM_{2.5}$  difference in February 2020 was linearly decomposed into three parts. Although this linear decomposition was  
273 reasonable in China in the past few years, we must note that this approximation did not consider was lack of considering the  
274 meteorology-emission interactions, the product of the emission, the loss lifetime and particularly the sulfate-nitrate-ammonia  
275 thermodynamics (Cai et al., 2017), which brought some uncertainties. The actual emission reduction effect is considerable  
276 (Fig. 3d), in line with the increasingly strengthened emission reduction policies in recent years. When calculating the  $PM_{DR}$  in  
277 2020, we use the method of extrapolation. Although the result is consistent with others observational and numerical studies  
278 (Geng et al., 2020; Zhang et al., 2020; Zhou et al., 2019), it is still conjectures-estimated value rather than true values. These

279 issues need to be examined in the future studies to unlock respective effects of emissions and meteorological conditions on  
280  $PM_{2.5}$  over eastern China. To restrict the possible uncertainties, we set up some constraints: 1. The pivotal contribution ratio of  
281 changing meteorology were calculated under two emission levels and recalculated by statistical regressed model; 2. The values  
282 of  $PM_{dM}$  and  $PM_{dR}$  were widely compared to previous studies.

283 If the COVID-19 epidemic did not occurred, the concentrations of  $PM_{2.5}$  would increase up to 1.3–1.7 times the  
284 observations in February 2020 (Fig. 7~~6~~). Therefore, the pollution abatement must continue. Because of the huge population  
285 base in the east of China, the anthropogenic emissions exceeded the atmospheric environmental capacity even during COVID-  
286 19 quarantines. Although the  $PM_{2.5}$  dropped much, marked air pollutions also occurred during this unique experiments that the  
287 human emissions were sharply closed. This raised new scientific questions, such as changes of atmospheric heterogeneous  
288 reactions and oxidability under extreme emission control, quantitative meteorology-emission interactions, and so on. This also  
289 implied reconsiderations of policy for pollution controls and necessity to cut off secondary productions of particulate matters  
290 basing on sufficient scientific research (Le et al., 2020; Huang et al., 2020). Some studies estimated that thousands of deaths  
291 were prevented during the quarantine because of the air pollution decrease (Chen K. et al., 2020). However, medical systems  
292 were still overstressed, and transportation to hospitals also decreased. Furthermore, the deaths related to air pollution were  
293 almost all due to respiratory diseases (Wang et al., 2001), and their corresponding medical resources were also further stressed  
294 by COVID-19. Therefore, the mortality impacted by the air pollution reduction during the COVID-19 outbreak should be  
295 comprehensively assessed in future work.

296 **Data availability.** Monthly mean meteorological data are obtained from ERA5 reanalysis data archive:  
297 <https://cds.climate.copernicus.eu/cdsapp#!/search?type=dataset>.  $PM_{2.5}$  concentration data are acquired from the China  
298 National Environmental Monitoring Centre: <http://beijingair.sinaapp.com/>. The emissions data of 1985 can be downloaded  
299 from <http://geoschemdata.computecanada.ca/ExtData/HEMCO/AnnualScalar/>, and that of 2010 can be obtained from MIX:  
300 <http://geoschemdata.computecanada.ca/ExtData/HEMCO/MIX>.

### 301 **Acknowledgements**

302 The National Natural Science Foundation of China (41991283, 9174431 and 41705058), the funding of Jiangsu innovation &  
303 entrepreneurship team, and the special project “the impacts of meteorology on large-scale spread of influenza virus” from CIC-  
304 FEMD supported this research.

### 305 **Authors' contribution**

306 Wang H. J. and Yin Z. C. designed and performed researches. Zhang Y. J. simulated the  $PM_{2.5}$  by GEOS-Chem model and Li

307 Y. Y. did the statistical analysis. Yin Z. C. prepared the manuscript with contributions from all co-authors.

## 308 **Competing interests**

309 The authors declare no conflict of interest.

## 310 **References**

311 Bey, I., Jacob, D. J., Yantosca, R. M., Logan, J. A., Field, B. D., Fiore, A. M., Li, Q. B., Liu, H. G. Y., Mickley, L. J., and  
312 Schultz, M. G.: Global modeling of tropospheric chemistry with assimilated meteorology: Model description and evaluation,  
313 *J. Geophys. Res. Atmos.*, 106, 23073–23095, <https://doi.org/10.1029/2001jd000807>, 2001.

314 Cai, S., Wang, Y., Zhao, B., Wang S., Chang, X., and Hao, J.: The impact of the “Air Pollution Prevention and Control Action  
315 Plan” on PM<sub>2.5</sub> concentrations in Jing-Jin-Ji region during 2012–2020, *Sci. Total Environ.*, 580, 197–209, 2017.

316 Cao, W., Fang, Z., Hou, G., Han, M., Xu X., and Dong, J.: The psychological impact of the COVID-19 epidemic on college  
317 students in China, *Psychiat. Res.*, 287, 112934, 2020.

318 Chen, S., Yang, J., Yang W., Wang, C., and Till, B.: COVID-19 control in China during mass population movements at New  
319 Year, *Lancet*, 395(10226), 764–766, 2020.

320 Chen, K., Wang, M., Huang, C., Patrick, L., and Paul, T.: Air Pollution Reduction and Mortality Benefit during the COVID-  
321 19 Outbreak in China, *MedRxiv*, <https://doi.org/10.1101/2020.03.23.20039842>, 2020.

322 Cleaner air for China, *Nat. Geosci.*, 12, 497–497, <https://doi.org/10.1038/s41561-019-0406-7>, 2019.

323 Dang, R., and Liao, H.: Severe winter haze days in the Beijing-Tianjin-Hebei region from 1985 to 2017 and the roles of  
324 anthropogenic emissions and meteorology, *Atmos. Chem. Phys.*, 19, 10801–10816, 2019.

325 Ding, Y., and Liu, Y.: Analysis of long-term variations of fog and haze in China in recent 50 years and their relations with  
326 atmospheric humidity, *Sci. China Ser. D.*, 57, 36–46, 2014.

327 Evans, M. J. and Jacob, D. J.: Impact of new laboratory studies of N<sub>2</sub>O<sub>5</sub> hydrolysis on global model budgets of  
328 tropospheric nitrogen oxides, ozone, and OH, *Geophys. Res. Lett.*, 32, L09813, <https://doi.org/10.1029/2005gl022469>,  
329 2005.

330 Fountoukis, C. and Nenes, A.: ISORROPIA II: a computationally efficient thermodynamic equilibrium model for K<sup>+</sup>-  
331 Ca<sup>2+</sup>-Mg<sup>2+</sup>-NH<sub>4</sub><sup>+</sup>-Na<sup>+</sup>-SO<sub>4</sub><sup>2-</sup>-NO<sub>3</sub><sup>-</sup>-Cl<sup>-</sup>-H<sub>2</sub>O aerosols, *Atmos. Chem. Phys.*, 7, 4639–4659, [https://doi.org/10.5194/acp-](https://doi.org/10.5194/acp-7-4639-2007)  
332 [7-4639-2007](https://doi.org/10.5194/acp-7-4639-2007), 2007.

333 Gelaro, R., McCarty, W., Suarez, M. J., Todling, R., Molod, A., Takacs, L., Randles, C. A., Darmenov, A., Bosilovich, M. G.,

334 Reichle, R., Wargan, K., Coy, L., Cullather, R., Draper, C., Akella, S., Buchard, V., Conaty, A., da Silva, A. M., Gu, W., Kim,

335 G. K., Koster, R., Lucchesi, R., Merkova, D., Nielsen, J. E., Partyka, G., Pawson, S., Putman, W., Rienecker, M., Schubert, S. D.,



336 Sienkiewicz, M., and Zhao, B.: The Modern-Era Retrospective Analysis for Research and Applications, Version 2 (MERRA2),  
337 J. Climate, 30, 5419–5454, <https://doi.org/10.1175/jcli-d-160758.1>, 2017.

338 Geng, G., Xiao, Q., Zheng, Y., Tong, D., Zhang, Y., Zhang, X., Zhang, Q., He, H., and Liu, Y.: Impact of China’s Air Pollution  
339 Prevention and Control Action Plan on PM<sub>2.5</sub> chemical composition over eastern China, Sci. China Ser. D., 62, 1872–1884,  
340 <https://doi.org/10.1007/s11430-018-9353-x>, 2020.

341 Huang, X., Ding, A., Gao, J., Zheng, B., Zhou, D., Qi, X., Tang, R., Ren, C., Nie, W., Chi, X., Wang, J., Xu, Z., Chen, L., Li,  
342 Y., Che, F., Pang, N., Wang, H., Tong, D., Qin, W., Cheng, W., Liu, W., Fu, Q., Chai, F., Davis, S., Zhang, Q., and He, K.:  
343 Enhanced secondary pollution offset reduction of primary emissions during COVID-19 lockdown in China, Natl. Sci. Rev.,  
344 nwa 137, 2020.

345 Jacob, D. J.: Heterogeneous chemistry and tropospheric ozone, Atmos. Environ., 34, 2131–2159,  
346 [https://doi.org/10.1016/s1352-2310\(99\)00462-8](https://doi.org/10.1016/s1352-2310(99)00462-8), 2000.

347 Kalnay, E., Kanamitsu, M., Kistler, R., Collins, W., Deaven, D., Gandin, L., Iredell, M., Saha, S., White, G., Woollen, J., Zhu,  
348 Y., Leetmaa, A., Reynolds, R., Chelliah, M., Ebisuzaki, W., Higgins, W., Janowiak, J., Mo, K. C., Ropelewski, C., Wang, J.,  
349 Jenne, R., and Joseph, D.: The NCEP/NCAR 40-year reanalysis project, B. Am. Meteorol. Soc., 77, 437–471,  
350 [https://doi.org/10.1175/1520-0477\(1996\)077<0437:TNYRP>2.0.CO;2](https://doi.org/10.1175/1520-0477(1996)077<0437:TNYRP>2.0.CO;2), 1996.

351 Kodros, J. K., Pierce, J. R.: Important global and regional differences in cloud-albedo aerosol indirect effect estimates between  
352 simulations with and without prognostic aerosol microphysics, J. Geophys. Res., 122, <https://doi.org/10.1002/2016JD025886>, 2017.

353 Le, T., Wang, Y., Liu, L., Yang, J., Yung, Y. L., Li, G., and John, H.: Unexpected air pollution with marked emission reductions  
354 during the covid-19 outbreak in China, Science, 369(6504), eabb7431, 2020.

355 Li, M., Zhang, Q., Kurokawa, J.-I., Woo, J.-H., He, K., Lu, Z., Ohara, T., Song, Y., Streets, D. G., Carmichael, G. R., Cheng,  
356 Y., Hong, C., Huo, H., Jiang, X., Kang, S., Liu, F., Su, H., and Zheng, B.: MIX: a mosaic Asian anthropogenic emission  
357 inventory under the international collaboration framework of the MICS-Asia and HTAP, Atmos. Chem. Phys., 17, 935–963,  
358 <https://doi.org/10.5194/acp-17-935-2017>, 2017.

359 Lian, X., Huang, J., Huang, R., Liu, C., and Zhang, T.: Impact of city lockdown on the air quality of COVID-19-hit of Wuhan  
360 city, Sci. Total Environ., 742, 140556, 2020.

361 Luo, Z.: The impact of new outbreak on economy, capital market and national governance and its response, Finance Economy,  
362 2020(2), 8–15, 2020.

363 Ministry of Environmental Protection of China.  
364 [http://www.mee.gov.cn/xxgk/2018/xxgk/xxgk05/201903/t20190306\\_694550.html](http://www.mee.gov.cn/xxgk/2018/xxgk/xxgk05/201903/t20190306_694550.html), 2019.

365 Niu, F., Li, Z., Li, C., Lee, K., and Wang, M.: Increase of wintertime fog in China: Potential impacts of weakening of the  
366 Eastern Asian monsoon circulation and increasing aerosol loading, J. Geophys. Res., 115, D7, 2020.

367 Park, R.: Natural and transboundary pollution influences on sulfate-nitrate-ammonium aerosols in the United States:  
12 / 21

368 Implications for policy, *J. Geophys. Res. Atmos.*, 109, D15204, 2004.

369 Shi, X., and Brasseur, G.: The Response in Air Quality to the Reduction of Chinese Economic Activities during the COVID  
370 Outbreak, *Geophys. Res. Lett.*, 2020, 47, 2020.

371 Shi, Y., Hu, F., Lü R., and He, Y.: Characteristics of urban boundary layer in heavy haze process based on beijing 325m tower  
372 data, *Atmos. Oceanic Sci. Lett.*, 12, 41–49, 2019.

373 Song, L., Wang, L., Chen, W., and Zhang, Y.: Intraseasonal Variation of the Strength of the East Asian Trough and Its  
374 Climatic Impacts in Boreal Winter, *J. Climate*, 29 (7), 2557–2577, <https://doi.org/10.1175/JCLI-D-14-00834.1>, 2016.

375 Sun, Y., Lei, L., Zhou, W., Chen, C., and Worsnop, D. R.: A chemical cocktail during the COVID-19 outbreak in Beijing,  
376 China: Insights from six-year aerosol particle composition measurements during the Chinese New Year holiday. *Sci. Total*  
377 *Environ.*, 140739, 2020.

378 Thornton, J. A., Jaegle, L., and McNeill, V. F.: Assessing known pathways for HO<sub>2</sub> loss in aqueous atmospheric aerosols:  
379 Regional and global impacts on tropospheric oxidants, *J. Geophys. Res.-Atmos.*, 113, D05303,  
380 <https://doi.org/10.1029/2007jd009236>, 2008.

381 Tian, H., Liu, Y., Li, Y., Wu, C., Chen, B., Kraemer, M., Li, B., Cai, J., Xu, B., Yang, Q., Wang, B., Yang, P., Cui, Y., Song, Y.,  
382 Zheng, P., Wang, Q., Bjornstad, O., Yang, R., Grenfell, B., Pybus, O., Dye, C.: An investigation of transmission control  
383 measures during the first 50 days of the COVID-19 epidemic in China, *Science*, eabb6105, 2020.

384 Wang, H., and Jin, Y.: The Study on Air Pollution Effects on the Mechanism of Respiratory System. *Science of Travel*  
385 *Medicine*, 007(002), 29–33, 2001.

386 Wang, P., Chen, K., Zhu, S., Wang, P., and Zhang, H.: Severe air pollution events not avoided by reduced anthropogenic  
387 activities during COVID-19 outbreak, *Resour. Conserv. Recy.*, 158, <http://doi:10.1016/j.resconrec.2020.104814>, 2020.

388 Wang, Y., Li, W., Gao, W., Liu, Z., Tian, S., Shen, R., Ji, D., Wang, S., Wang, L., Tang, G., Tao, S., Cheng, M., Wang, G., Gong,  
389 Z., Hao, J., and Zhang, Y.: Trends in particulate matter and its chemical compositions in China from 2013–2017, *Sci. China*  
390 *Ser. D.*, 62(12), 1857–1871, 2019.

391 Xia, J., and Feng, X.: Impacts of COVID-19 epidemic on tourism industry and related countermeasures, *Chinese Business and*  
392 *Market*, 34(3), 3–10, 2020.

393 Xiao, D., Li, Y., Fan, S., Zhang, R., Sun, J., and Wang, Y.: Plausible influence of Atlantic Ocean SST anomalies on winter haze  
394 in China. Plausible influence of Atlantic Ocean SST anomalies on winter haze in China, *Theor. Appl. Climatol.*, 122, 249–257,  
395 2015.

396 Yang, Y., Liao, H., and Lou, S.: Increase in winter haze over eastern China in recent decades: Roles of variations in  
397 meteorological parameters and anthropogenic emissions, *J. Geophys. Res. Atmos.*, 121, 13050–  
398 13065, <https://doi.org/10.1002/2016jd025136>, 2016.

399 Yin, Z., and Wang, H.: The relationship between the subtropical Western Pacific SST and haze over North-Central North China

400 Plain, *Int. J. Climatol.*, 36, 3479–3491, 2016.

401 Yin, Z., and Wang, H.: Role of atmospheric circulations in haze pollution in December 2016, *Atmos. Chem. Phys.* 17, 11673–  
 402 11681. <https://doi.org/10.5194/acp-17-11673-2017> , 2017.

403 Yin, Z., Wang, H., and Guo, W.: Climatic change features of fog and haze in winter over North China and Huang-Huai Area,  
 404 *Sci. China Ser. D.*, 58, 1370–1376, 2015.

405 Yin, Z., and Zhang, Y.: Climate anomalies contributed to the rebound of PM<sub>2.5</sub> in winter 2018 under intensified regional air  
 406 pollution preventions, *Sci. Total Environ.*, 726, 138514, 2020.

407 Yu, F., and Luo, G.: Simulation of particle size distribution with a global aerosol model: Contribution of nucleation to aerosol  
 408 and CCN number concentrations, *Atmos. Chem. Phys.*, 9, 7691-7710, 2009.

409 Zhang, X., Xu, X., Ding, Y., Liu, Y., Zhang, H., Wang, Y., Zhong, J.: The impact of meteorological changes from 2013 to 2017  
 410 on PM<sub>2.5</sub> mass reduction in key regions in China, *Sci. China Ser. D.*, 62, 1885–1902, [https://doi.org/10.1007/s11430-019-9343-](https://doi.org/10.1007/s11430-019-9343-3)  
 411 3, 2020.

412 Zhou, W., Gao, M., He, Y., Wang, Q., Xie, C., Xu, W., Zhao, J., Du, W., Qiu, Y., Lei, L., Fu, P., Wang, Z., Worsnop, D., Zhang,  
 413 Q., and Sun, Y.: Response of aerosol chemistry to clean air action in Beijing, China: Insights from two-year ACSM  
 414 measurements and model simulations, *Environ. Pollut.*, 255, 113345, 2019.

415 Zou, Y., Wang, Y., Zhang, Y., and Koo, J.: Arctic sea ice, Eurasia snow, and extreme winter haze in China, *Sci. Adv.*, 3,  
 416 e1602751, 2017.

## 417 **Figure Captions**

418 Figure 1. (a) Variation in existing confirmed cases (bar; red: increase, blue: decrease) and the ratio of accumulated confirmed  
 419 cases to total confirmed cases (black line) in China. (b) The ratio of work resumption in large industrial enterprises in the east  
 420 of China. (c) Time of the official 7-days holiday of Chinese New Year from 2013 to 2020.

421 Figure 2. (a) Spatial distribution of observed (dots) and GEOS-Chem simulated (shading) PM<sub>2.5</sub> (unit:  $\mu\text{g}/\text{m}^3$ ) in February  
 422 2017. Observed PM<sub>2.5</sub> concentrations (black, unit:  $\mu\text{g}/\text{m}^3$ ) and simulated PM<sub>2.5</sub> concentrations under 2010 emission (red) and  
 423 1985 emission (blue) in February 2020 in (b) North China (NC), (c) Yangtze River Delta (YRD) and (d) Hubei Province (HB).

424 Figure 3. Differences in the observed PM<sub>2.5</sub> (unit:  $\mu\text{g}/\text{m}^3$ ) in February between 2020 and 2017. The black boxes indicate the  
 425 locations of North China (NC, 32.5-42°N, 110-120°E), the Yangtze River Delta (YRD, 28-32.5°N, 118-122°E) and Hubei  
 426 Province (HB, 30-32.5°N, 109.5-116°E). ~~Figure 3. PM<sub>2.5</sub> difference (unit:  $\mu\text{g}/\text{m}^3$ ) in February between 2020 and 2017 due to~~  
 427 ~~(a) changing meteorology (PMd<sub>M</sub>), (b) expected routine emission reductions (PMd<sub>R</sub>), (c) the COVID-19 quarantines (PMd<sub>C</sub>),~~  
 428 ~~and (d) due to the total emission reduction (PMd<sub>E</sub> = PMd<sub>R</sub> + PMd<sub>C</sub>).~~

429 Figure 4. Differences in the observed atmospheric circulation in February between 2020 and 2017, including (a) geopotential

430 potential height at 500 hPa (unit: gpm), (b) wind at 850 hPa (arrows; unit: m/s), surface relative humidity (shading; unit: %).  
431 The atmospheric circulations in the stagnant days (e.g., from 8–13 and 19–25 February 2020) were also showed, including (c)  
432 geopotential potential height at 500 hPa (shading; unit: gpm) and its climate mean in February (contour), and (d) wind at 850  
433 hPa (black arrows; unit: m/s), its climate mean (blue arrows) and the increased surface relative humidity (shading; unit: %, stagnant days minus climate mean).

435 Figure 53.  $PM_{2.5}$  difference (unit:  $\mu g/m^3$ ) in February between 2020 and 2017 due to (a) changing meteorology ( $PMd_M$ ), (b)  
436 expected routine emission reductions ( $PMd_R$ ), (c) the COVID-19 quarantines ( $PMd_C$ ), and (d) due to the total emission  
437 reduction ( $PMd_E = PMd_R + PMd_C$ ).

438 Figure 65. Variation in  $PMd_R$  (unit:  $\mu g/m^3$ ) with respect to the February 2017 level in Beijing, Shanghai and Wuhan from 2015  
439 to 2019.  $PMd_R$  in 2020 was linearly extrapolated from that in the 2015–2019 period. The dotted line is the linear trend.

440 Figure 76. Contributions of  $PMd_M$  (orange bars with hatching),  $PMd_R$  (purple bars with hatching) and  $PMd_C$  (blue bars with  
441 hatching) to the change in  $PM_{2.5}$  concentration (unit:  $\mu g/m^3$ ) between 2020 and 2017 in the three regions. The observed  $PM_{2.5}$   
442 concentration in February 2017 (black) and 2020 (gray) was also plotted, and the expected  $PM_{2.5}$  concentration without the  
443 COVID-19 quarantine is indicated by black hollow bars. The contribution ratios of the three factors (relative to the  $PM_{2.5}$   
444 observations in 2020) are also indicated on the corresponding bars.

445 Figure 87. (a) Differences in the observed  $PM_{2.5}$  (unit:  $\mu g/m^3$ ) in March between 2020 and 2017. (b) Contributions of  $PMd_C$   
446 to the change in  $PM_{2.5}$  concentration (unit:  $\mu g/m^3$ ) between 2020 and 2017 and (c) the contribution ratios of  $PMd_C$  (relative to  
447 the  $PM_{2.5}$  observations in 2020) in March (blue) and February (red) in the three regions.

448

449

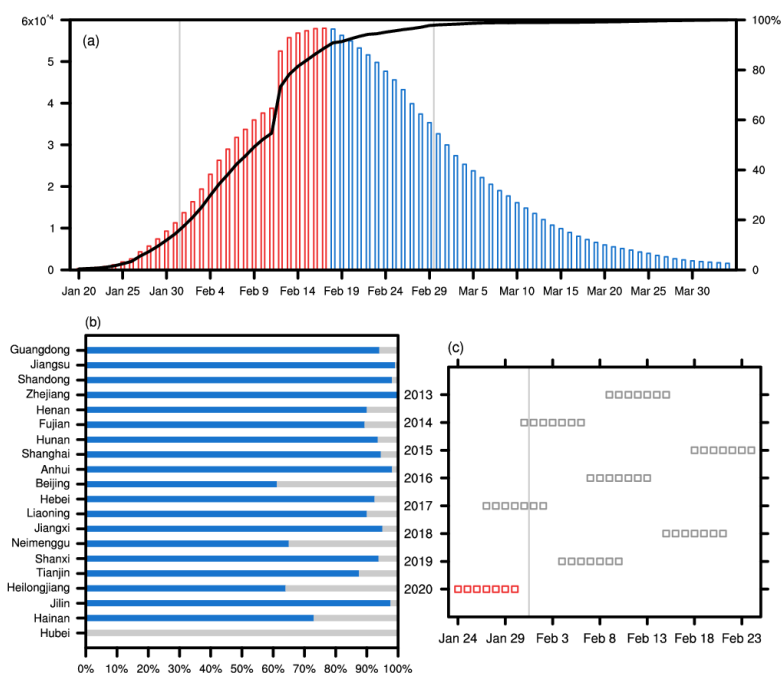
450

451

452

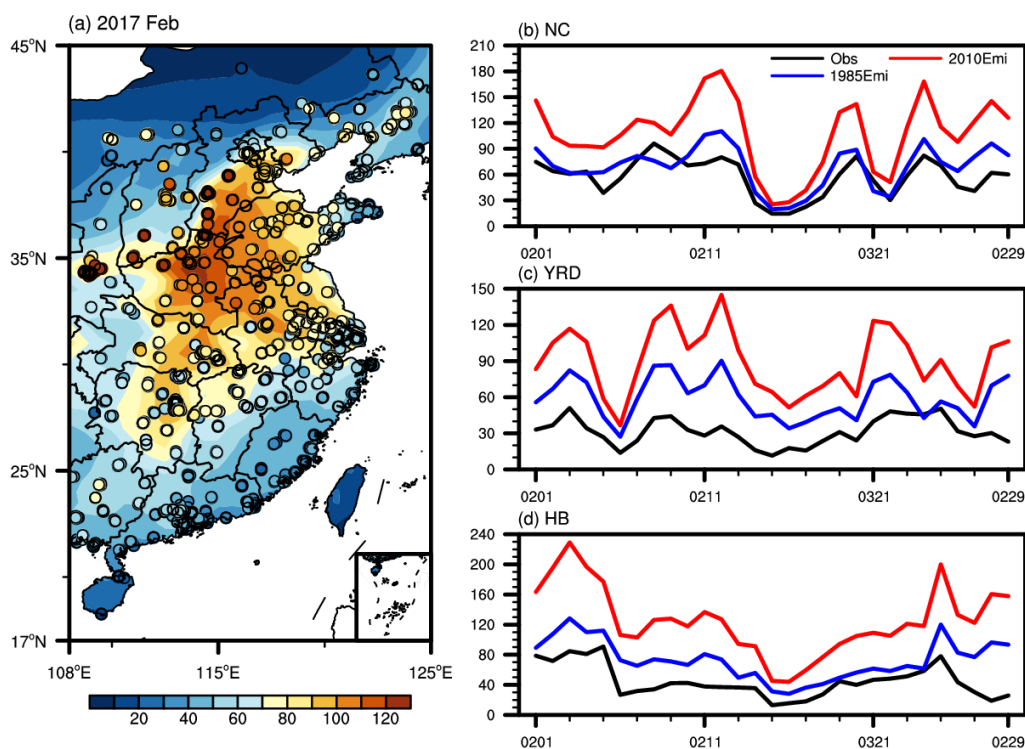
453

454



457

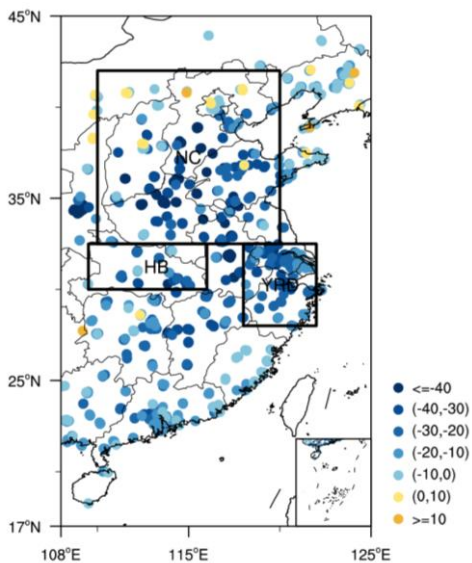
458 **Figure 1.** (a) Variation in existing confirmed cases (bar; red: increase, blue: decrease) and the ratio of accumulated confirmed  
 459 cases to total confirmed cases (black line) in China. (b) The ratio of work resumption in large industrial enterprises in the east  
 460 of China until the end February. (c) Time of the official 7-days holiday of Chinese New Year from 2013 to 2020.



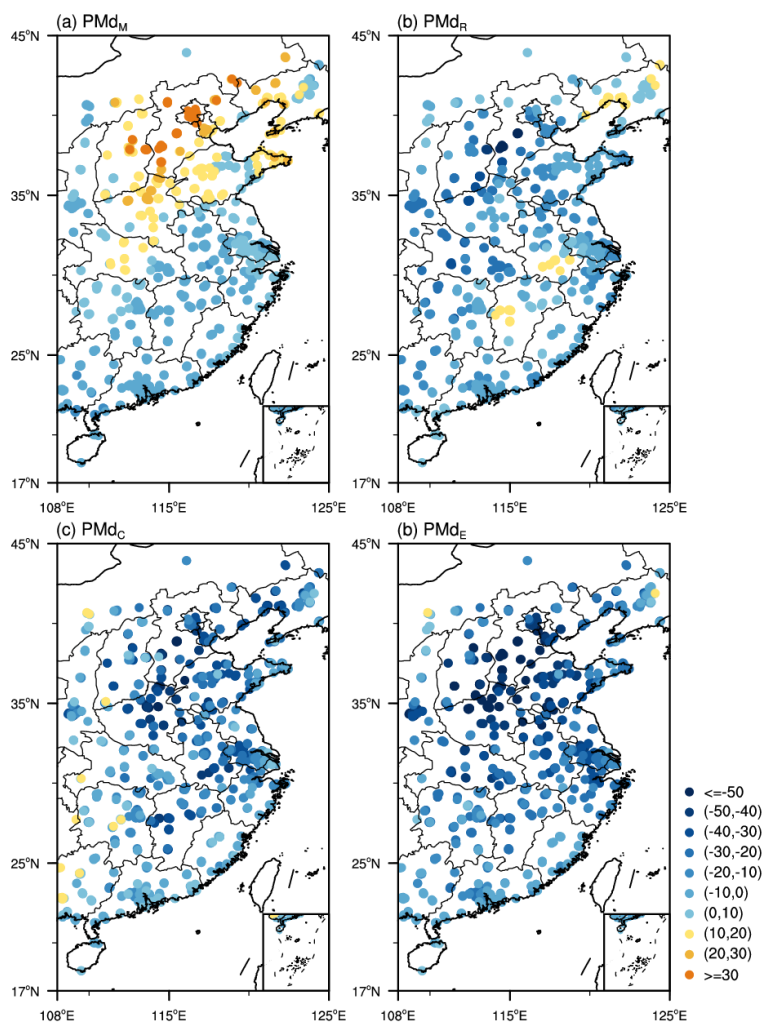
461

462 **Figure 2.** (a) Spatial distribution of observed (dots) and GEOS-Chem simulated (shading)  $PM_{2.5}$  (unit:  $\mu g/m^3$ ) in February

463 2017. Observed  $PM_{2.5}$  concentrations (black, unit:  $\mu g/m^3$ ) and simulated  $PM_{2.5}$  concentrations under 2010 emission (red) and  
 464 1985 emission (blue) in February 2020 in (b) North China (NC), (c) Yangtze River Delta (YRD) and (d) Hubei Province (HB).

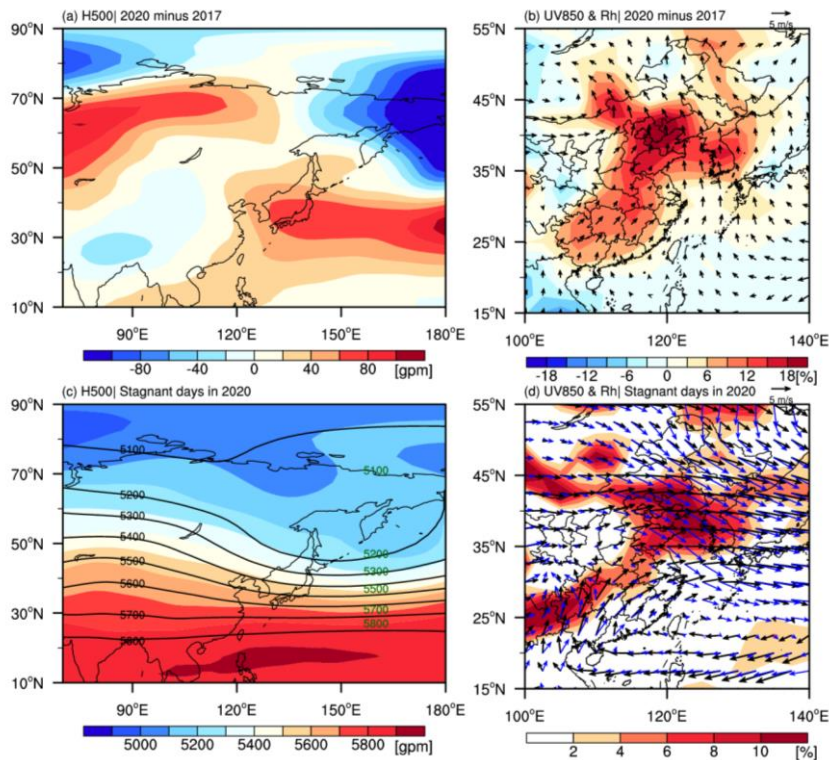


465  
 466 **Figure 32.** Differences in the observed  $PM_{2.5}$  (unit:  $\mu g/m^3$ ) in February between 2020 and 2017. The black boxes indicate the  
 467 locations of North China (NC, 32.5-42°N,110-120°E), the Yangtze River Delta (YRD, 28-32.5°N,118-122°E) and Hubei  
 468 Province (HB, 30-32.5°N,109.5-116°E).



470 ~~Figure 3.  $PM_{2.5}$ -difference (unit:  $\mu g/m^3$ ) in February between 2020 and 2017 due to (a) changing meteorology ( $PMd_M$ ), (b)~~  
 471 ~~expected routine emission reductions ( $PMd_R$ ), (c) the COVID-19 quarantines ( $PMd_C$ ), and (d) due to the total emission~~  
 472 ~~reduction ( $PMd_E = PMd_R + PMd_C$ ).~~

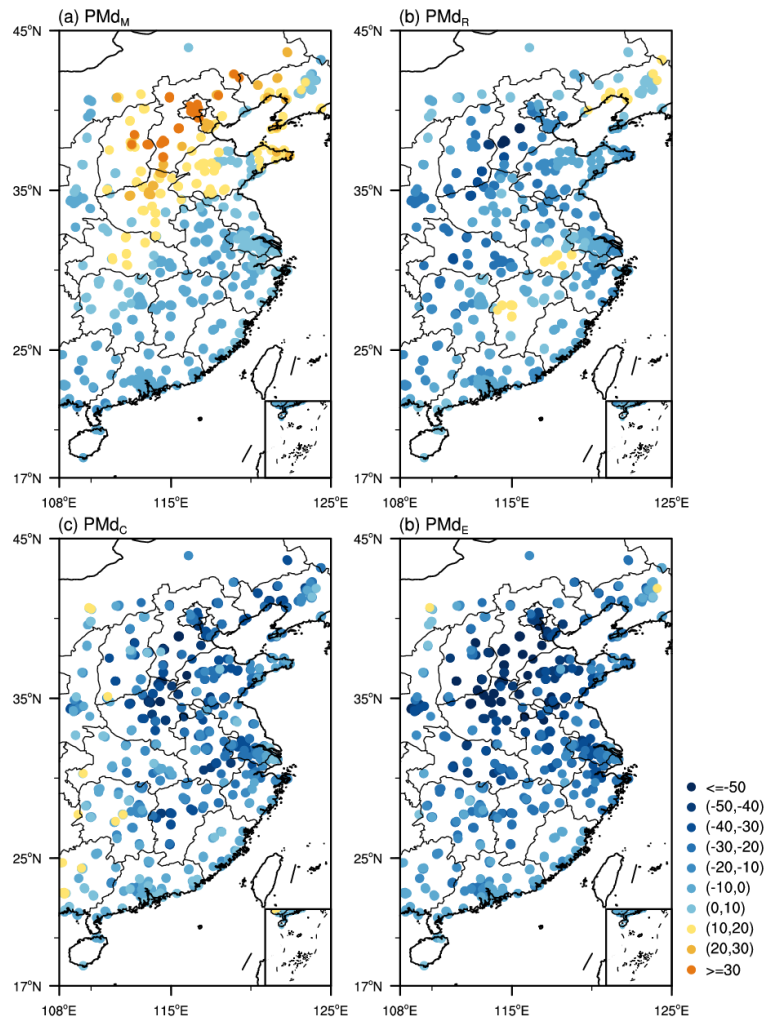
473



474

475 **Figure 4.** Differences in the observed atmospheric circulation in February between 2020 and 2017, including (a) geopotential  
 476 potential height at 500 hPa (unit: gpm), (b) wind at 850 hPa (arrows; unit: m/s), surface relative humidity (shading; unit: %).  
 477 The atmospheric circulations in the stagnant days (e.g., from 8–13 and 19–25 February 2020) were also showed, including (c)  
 478 geopotential potential height at 500 hPa (shading; unit: gpm) and its climate mean in February (contour), and (d) wind at 850  
 479 hPa (black arrows; unit: m/s), its climate mean (blue arrows) and the increased surface relative humidity (shading; unit: %, stagnant days minus climate mean).

480



481

482

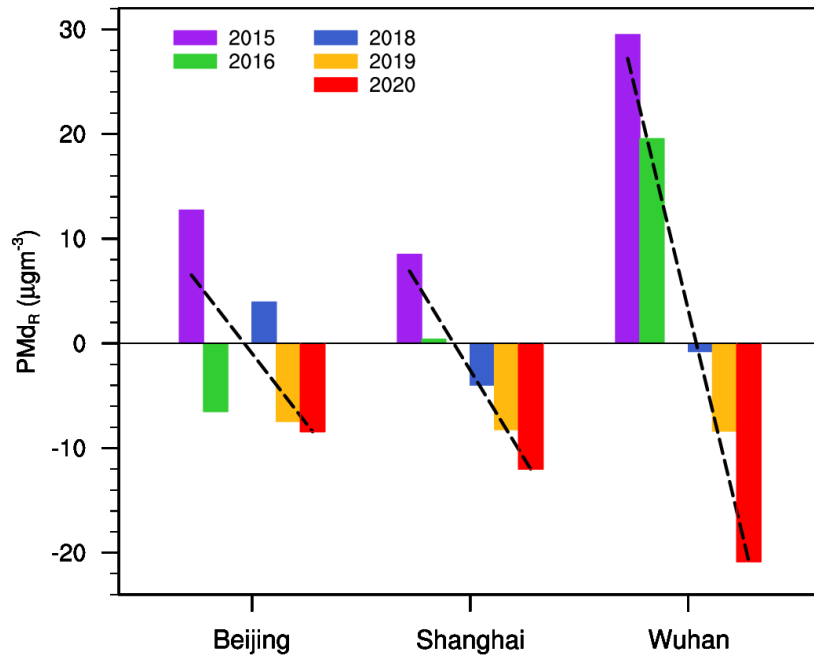
483

484

485

**Figure 53.**  $PM_{2.5}$  difference (unit:  $\mu g/m^3$ ) in February between 2020 and 2017 due to (a) changing meteorology ( $PMd_M$ ), (b) expected routine emission reductions ( $PMd_R$ ), (c) the COVID-19 quarantines ( $PMd_C$ ), and (d) due to the total emission reduction ( $PMd_E = PMd_R + PMd_C$ ).



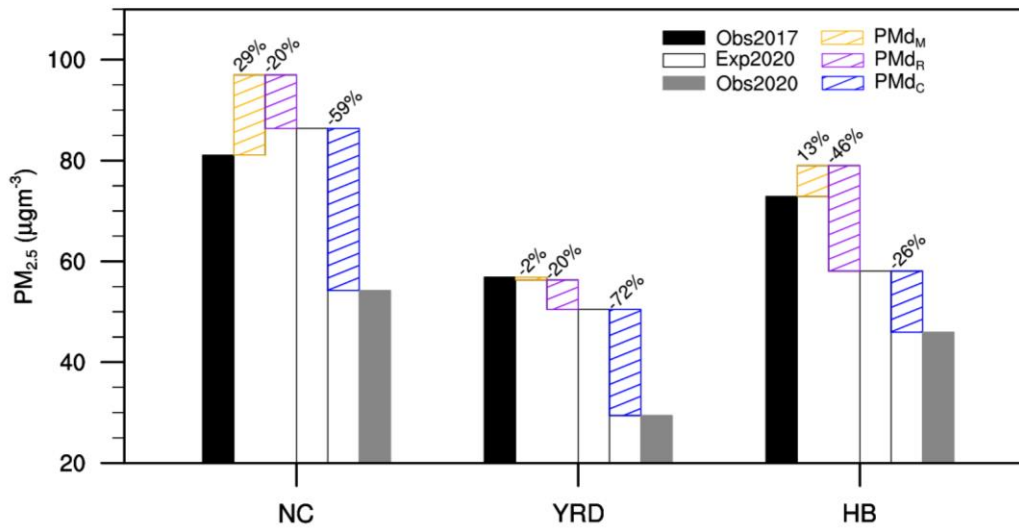


486

487

488

**Figure 56.** Variation in  $\text{PMd}_R$  (unit:  $\mu\text{g}/\text{m}^3$ ) with respect to the February 2017 level in Beijing, Shanghai and Wuhan from 2015 to 2019.  $\text{PMd}_R$  in 2020 was linearly extrapolated from that in the 2015–2019 period. The dotted line is the linear trend.



489

490

491

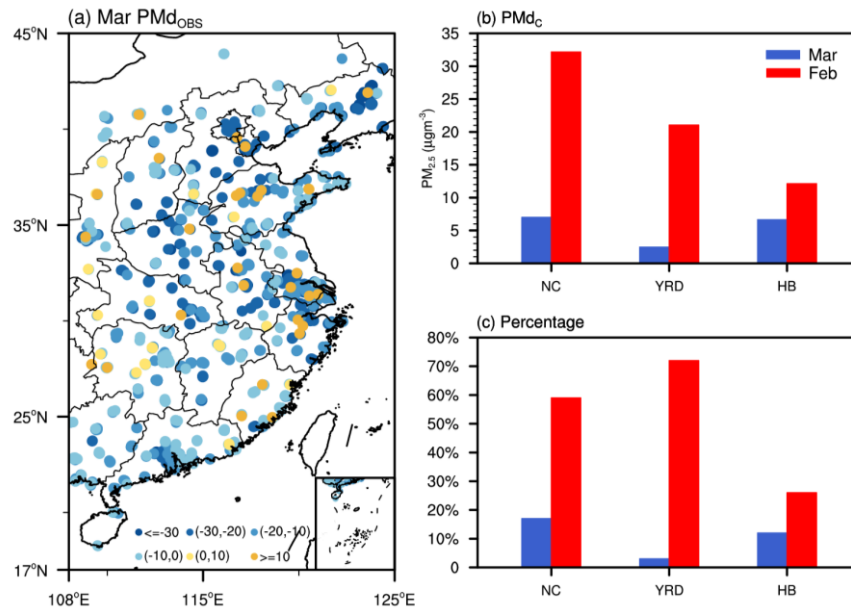
492

493

494

495

**Figure 76.** Contributions of  $\text{PMd}_M$  (orange bars with hatching),  $\text{PMd}_R$  (purple bars with hatching) and  $\text{PMd}_C$  (blue bars with hatching) to the change in  $\text{PM}_{2.5}$  concentration (unit:  $\mu\text{g}/\text{m}^3$ ) between 2020 and 2017 in the three regions. The observed  $\text{PM}_{2.5}$  concentration in February 2017 (black) and 2020 (gray) was also plotted, and the expected  $\text{PM}_{2.5}$  concentration without the COVID-19 quarantine is indicated by black hollow bars. The contribution ratios of the three factors (relative to the  $\text{PM}_{2.5}$  observations in 2020) are also indicated on the corresponding bars.



496

497

498

499

500

501

**Figure 87.** (a) Differences in the observed PM<sub>2.5</sub> (unit: μg/m<sup>3</sup>) in March between 2020 and 2017. (b) Contributions of PM<sub>dC</sub> to the change in PM<sub>2.5</sub> concentration (unit: μg/m<sup>3</sup>) between 2020 and 2017 and (c) the contribution ratios of PM<sub>dC</sub> (relative to the PM<sub>2.5</sub> observations in 2020) in March (blue) and February (red) in the three regions.